JOURNAL OF NANO- AND ELECTRONIC PHYSICS
Vol. 8 No 4, 04019(4pp) (2016)

ЖУРНАЛ НАНО- ТА ЕЛЕКТРОННОЇ ФІЗИКИ
Том 8 № 4, 04019(4cc) (2016)

Formation of a Nanostructured Coating Based on the Amorphous Carbon Matrix and Silver Nanocrystallites

A.Ya. Kolpakov[1], A.I. Poplavsky[1], S.S. Manokhin[1], M.E. Galkina[1], I.Yu. Goncharov[1], R.A. Liubushkin[1], J.V. Gerus[1], P.V. Turbin[2,3], L.V. Malikov[2,3]

[1] *Belgorod State National Research University, 85, Pobedy St., 308015 Belgorod, Russian Federation*
[2] *V.N. Karazin Kharkiv National University, 4, Svobody sq., 61022 Kharkiv, Ukraine,*
[3] *Scientific Center of Physical Technologies of MES and NAS of Ukraine, 6, Svobody sq., 61022 Kharkiv, Ukraine*

(Received 10 October 2016; published online 29 November 2016)

A nanostructured coating based on the amorphous carbon matrix and silver nanocrystallites (nanoclusters) is obtained by pulsed vacuum-arc deposition method. It is found that instantaneous coating formation rate influences the sizes and amount of silver nanoclusters. The effect of the local inhomogeneous distribution density of silver nanoclusters and their coalescence at the initial stage of the coating formation are observed. The features of a separate silver nanocrystallite crystal structure were investigated using a high-resolution transmission electron microscopy. The electron energy loss spectra in the region of the amorphous carbon matrix and silver nanocrystallites location region, as well as the Raman spectra were obtained. Some promising applications of a nanostructured carbon coating doped with silver have been proposed.

Keywords: Amorphous carbon nanoclusters, Nanostructured coatings, Raman spectroscopy, Silver.

DOI: 10.21272/jnep.8(4(1)).04019 PACS numbers: 81.05.U –, 81.05.Uw, 81.05.Zx

1. INTRODUCTION

The properties of hard carbon coatings with a high content of the sp^3-phase or ta-C coatings [1] obtained on a cold substrate from a stream of accelerated particles or carbon ions, largely coinciding with the properties of diamond, determine their application areas in metalworking, machine parts, micromechanical products, IR optics, as well as in medicine, where they are used to increase the biocompatibility of implants [2]. Silver nanoparticles in themselves also have special features, namely, antibacterial properties, unique optical characteristics, etc. [3]. A number of works present the successful attempts to combine the properties of these materials (amorphous carbon and silver nanoparticles). In particular, the properties of carbon coatings doped with silver and obtained by pulsed laser deposition method, which are the carbon matrix with silver nanoclusters are shown. It is established that these coatings have antimicrobial properties [4]. The results of studies of the structure and biomedical characteristics of DLC (diamond-like carbon) doped with silver obtained by pulsed vacuum-arc method with plasma flow filtration are presented in [5]. The dependence of the structure of these coatings on the accelerating potential applied to the substrate is determined. The coatings have high hemocompatibility. The characteristics of nanocomposite carbon coatings obtained by different methods and silver doped were investigated by XPS and AFM techniques; the smoothing effect of a silver-doped carbon coating is established [6]. The Ag-DLC multilayer coatings produced by magnetron sputtering method were tested for the stability of individual layers depending on their thickness; the growth effect of silver nanoclusters caused by their coalescence is defined [7].

Further studies aimed at determining the ways to influence the properties of this unique object, namely, the size and amount of silver nanoparticles, as well as the surface morphology are of interest. Here, it is necessary to consider the basic mechanisms of the formation of nanostructures in the coatings: self-organization of the coating structure under the influence of temperature and internal stress fields; the formation of the coating structure under the influence of ion bombardment of its surface, as well as the clustering (coalescence) of the doping element particles in the carbon coating due to the interaction energy between the matrix and the doping element depending on the density of the carbon flux entering the substrate. In this respect, the pulsed vacuum-arc method allowing to generate a pulsed plasma with high density expands the possibilities of methods for producing nanostructured coatings based on carbon and silver.

2. EXPERIMENTAL

The deposition of carbon coatings with the addition of silver of 10-200 nm thick was performed on a modified UVNIPA-1-001 setup equipped with a pulsed carbon plasma source with a consumable graphite cathode [8] made of MPG-6 graphite with cylindrical silver inserts of 3 and 10 mm in diameter. An ion source of the type II-4-0.15 was utilized to pre-clean the substrate with argon ions. The coatings of 10-50 nm thick were deposited on a fresh cleavage of a NaCl single-crystal for study by transmission electron microscopy methods. The coatings of 10, 50 and 200 nm thick were deposited on polished silicon for investigation by scanning probe microscopy and Raman spectroscopy methods. The coatings deposited on a NaCl single crystal were separated from the substrate in distilled water by the standard procedure. The samples on silicon of 10, 50 and 200 nm thick were annealed in a GHA 10/600 vacuum furnace (Carbolite Co.) at a temperature of 600 °C for 10 minutes. The coating deposition rate was equal to 0.01 nm/pulse for the cathode with a silver insert of 10 mm and 0.1 nm/pulse – with a 3 mm insert. To study the coating morphology and electronic structure, high-resolution transmission electron microscopy (HRTEM) methods were used with a Tecnai G2 F20 S-TWIN transmission electron microscope. The elemental composition of the coatings was investigated by the energy dispersive X-ray (EDX) spectroscopy method. The

coating thickness was determined on the transverse cleavages using a NOVA NANOSEM scanning electron microscope; a NTEGRA AURA scanning probe microscope was utilized to study the relief of nanosized carbon coatings. The Raman spectra were obtained using a LabRam HR Raman confocal microspectrometer at a laser emission wavelength of 532 nm.

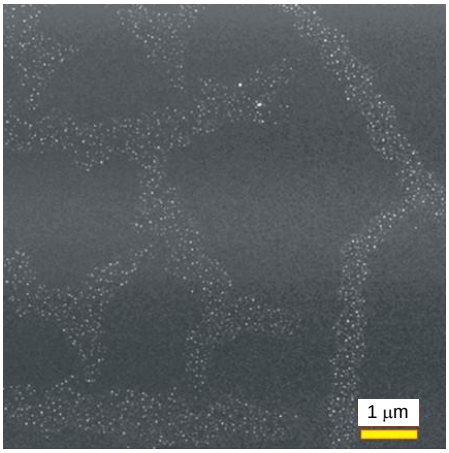

a

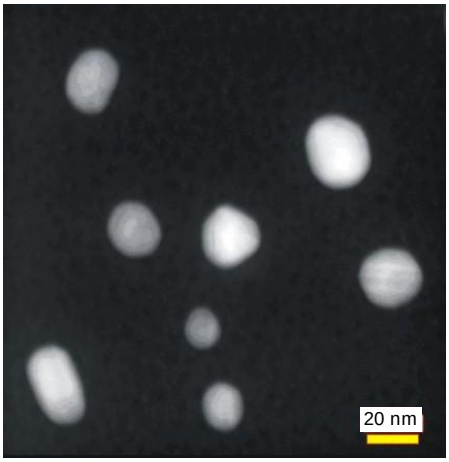

b

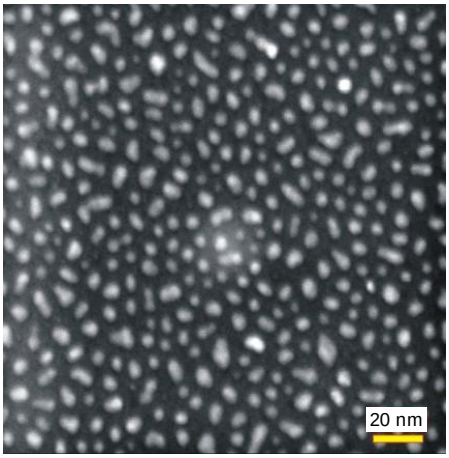

c

Fig. 1 – Electron microscopic image of the 10 nm thick coating obtained at a coating formation rate of 0.1 nm/pulse. General view of the coating (a), region 1 at a magnification of × 640000 (b) and region 2 at a magnification of × 640000 – (c)

3. RESULTS OF THE STUDY

In Fig. 1 and Fig. 2 we illustrate the electron-microscopic images of the carbon coatings doped with silver of 10 nm thick and obtained at a coating formation rate of 0.1 nm/pulse and 0.01 nm/pulse. The silver content in these coatings is 9 % and 10 %, respectively. In Fig. 3 we show the high-resolution electron microscopic images of individual nanoclusters obtained in the above modes.

In Fig. 4 we present the partial electron energy loss spectrum for the a-C:Ag coatings of 10 and 50 nm thick obtained at a formation rate of 0.1 nm/pulse, as well as the spectrum obtained in the coating region located between the silver crystallites (a-C). The line 1 marks the center of the 1s-π a)* transition in graphite (285.3 eV), line 2 indicates the beginning of the 1s-σ* transition in

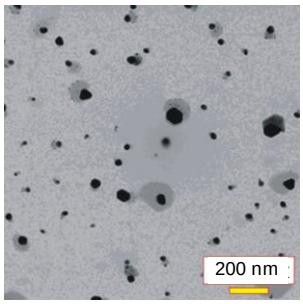

a

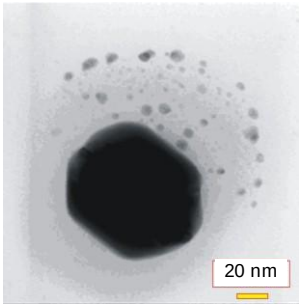

b

Fig. 2 – Electron microscopic image of the 10 nm thick coating obtained at a coating formation rate of 0.01 nm/pulse (a) and an individual nanocluster (b)

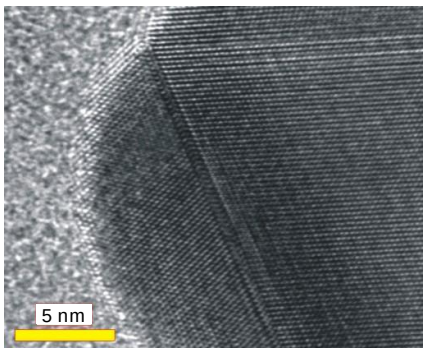

a

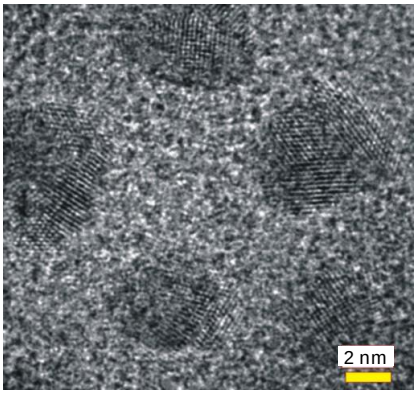

b

Fig. 3 – High-resolution electron microscopic image of silver nanoclusters in the carbon coating obtained at a coating formation rate of 0.01 nm/pulse (a) and 0.1 nm/pulse (b)

diamond (289.1 eV) and line 3 denotes the beginning of the 1s-σ* transition in graphite (291.7 eV) [9]. The average value of the plasmon energy for the a-C:Ag samples is 26.2 eV. In the local region of amorphous carbon a-C between coarse Ag crystallites, the average value of the plasmon energy is 27.5 eV. For the local region of amorphous carbon a-C between Ag crystallites, the center of the 1s-π* transition (~ 284.8 eV) is located slightly to the left of the 1s-π* line of the graphite transition (line 1 in Fig. 4). It should be noted that the obtained spectrum of a-C is similar to the spectra of ta-C coatings [9].

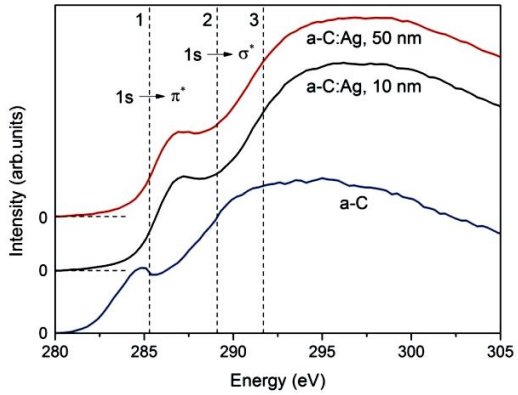

Fig. 4 – K-edge of carbon in the energy loss spectrum of a-C:Ag samples of 10 and 50 nm thick obtained at a formation rate of 0.1 nm/pulse. The a-C spectrum is taken from the local region of amorphous carbon between Ag crystallites. Line 1 indicates the center of the 1s-π*transition in graphite (285.3 eV), line 2 marks the beginning of the 1s-σ* transition in diamond (289.1 eV), and line 3 denotes the beginning of the 1s-σ* transition in graphite (291.7 eV) [9]

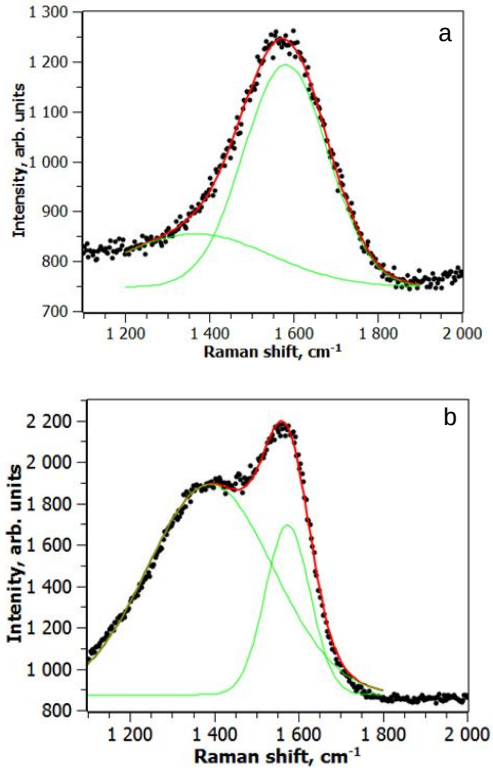

Fig. 5 – Raman spectra of the a-C:Ag coatings of 200 nm thick before (a) and after (b) annealing in vacuum at a temperature of 600 ºC

Table 1 – Results of processing the spectra shown in Fig. 5

a-C:Ag (in the initial state)			
Peak	Center, cm^{-1}	I	I_D/I_G
D	1365	350	1.01
G	1543	345	
a-C:Ag (after annealing in vacuum t a temperature of 600 ºC)			
D	1391	1018	1.24
G	1574	821	

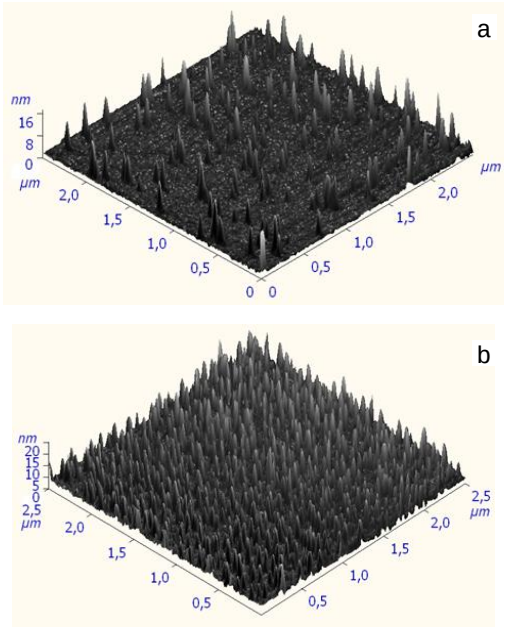

Fig. 6 – Volumetric image of the surface of a carbon coating of 20 nm (a) and 200 nm (b) thick

For the amorphous carbon matrix containing silver nanocrystallites a-C:Ag, the peak center of the 1s-π* transition (~ 287 eV) shifts to the right relative to the graphite transition line 1. The beginning of the 1s-σ* transition for a-C:Ag also lies to the right of a-C. The coating thickness in the range of 10-50 nm does not influence the electron energy loss spectrum.

In Fig. 5 we show the Raman spectra of the a-C:Ag coatings of 200 nm thick before and after annealing in vacuum at a temperature of 600 ºC. Table 1 presents the results of processing these spectra. We should note that electron energy loss spectroscopy (EELS) and the Raman spectra for the coatings obtained at a formation rate of 0.01 nm/pulse practically do not differ from those shown in Fig. 4 and Fig. 5.

Fig. 6 illustrates the scans of the silver-doped carbon coatings of 20 nm and 200 nm thick obtained by AFM.

The maximum height of the nano-projections of the 20 nm thick coating is equal to17 nm and of the 200 nm thick coating – 20 nm.

4. ANALYSIS AND DISCUSSION OF THE RESULTS

Analyzing the electron microscopic image of the 10 nm thick aC:Ag coating obtained at a coating formation rate of 0.1 nm/pulse (Fig. 1), it is necessary to note the presence of silver nanocluster local regions of a certain size coinciding with the emergence of dislocations and steps

on the substrate surface of a NaCl single crystal that indicates the influence of the substrate surface state on the size and distribution density of silver nanoclusters. This effect is associated with a reduced nucleation energy of silver nanoclusters on defects and, possibly, as a result of the coalescence of smaller clusters into coarse ones.

The formation rate of a coating based on silver-doped amorphous carbon affects the number and size of silver nanoclusters. The average size of silver nanoclusters obtained at a formation rate of 0.01 nm/pulse is 21 nm and at a formation rate of 0.1 nm/pulse – 55 nm. Moreover, the density of silver clusters in the matrix of amorphous carbon in the first case exceeds 8 times the corresponding index at a lower coating deposition rate.

The image of an individual nanocluster, near which smaller nanoclusters are observed (Fig. 2a, c), is of great interest. It can be assumed that the effect of coalescence takes place. In this case, namely, when plasma containing carbon and silver ions is condensed, three film growth mechanisms occur: first, the formation of an amorphous carbon film under non-equilibrium conditions (at a low substrate temperature and concomitant ion irradiation), second, the formation of silver islands from silver ions having a tighter binding between each other than with carbon matrix atoms and, finally, layer-by-layer growth of silver islands with an ordered crystal structure, which can be considered as nanoclusters. This could be viewed as a classical formation mechanism of nanostructures, such as quantum dots. Here, the dependence of the sizes and the number of nanoclusters on the supersaturation, in our case on the coating formation rate, corresponds to the well-established concepts.

Using HRTEM, it was possible to establish that nanoclusters had a crystal structure. The studied silver nanocrystallite illustrated in Fig. 3a has a face-centered cubic (fcc) lattice, the interplanar distances are in good agreement with the tabulated data for silver. The twinning effect, i.e. the formation in a single crystal of regions with a changed orientation of the crystal structure, takes place. This effect was also revealed for nanocrystallites shown in Fig. 3b, however, the degree of ordering of the nanocrystallite structure is smaller.

The analysis of EELS and the Raman spectra allows to conclude that the obtained results coincide with the data of other publications [5], namely, doping of a carbon coating with silver leads to a decrease in the sp^3-phase content in the aC:Ag coating that is clearly manifested in a characteristic change of the Raman spectrum after annealing in vacuum at a temperature of 600 ºC.

The AFM results make it possible to supplement the information obtained using electron microscopy methods, namely, to determine the time history of the height of the nano-projections and their number with increasing coating thickness, moreover, to define the relationship between the lateral size of the islands and their height. The most interesting result is the effect of a significant increase in the number of nano-projections with increasing carbon coating thickness from 20 to 200 nm, while the lateral sizes of the nano-projections and their height vary insignificantly.

Positive results of biomedical studies of the coatings based on the amorphous carbon matrix and silver nanocrystallites [10] show the prospects of their use in implants, in addition, it is possible to apply these coatings to create nano-membranes and biosensors.

5. CONCLUSIONS

1. The nature of the influence of the substrate on the size and distribution density of silver nanoclusters in the a-C:Ag coating is established.
2. It is shown that the formation rate of the coating based on silver-doped amorphous carbon affects the number and size of silver nanoclusters.
3. The formation mechanisms of the nanostructured a-C:Ag coating are determined.
4. The crystal structure of silver nanoclusters is determined.

ACKNOWLEDGEMENTS

This work has been performed under the financial support of the Russian Foundation for Basic Research (RFBR) and the administration of the Belgorod region under the Project No 15-48-03072 using the equipment of the Belgorod State University Common Use Centre for Diagnostics of Nanomaterials' Structure and Properties.

REFERENCES

1. I.V. Antonova, *Phys.-Usp.* 10, 1115 (2013).
2. D.R. Cooper, B. D'Anjou, N. Ghattamaneni, B. Harack, M. Hilke, A. Horth, N. Majlis, M. Massicotte, L. Vandsburger, E. Whiteway, *Eur. Phys. J. B* 86, 111 (2013).
3. W. Liu, H. Li, C. Xu, Y. Khatami, K. Banerjee, *Carbon* 49, 4122 (2011).
4. O.S. Kiselevskiy, V.P. Kazachenko, A.I. Yegorov, *Poverkhnost'. Rentgenovskiye, sinkhrotronnyye i neytronnyye issledovaniya* 2, 109 (2003).
5. I.N. Kolupaev, V.O. Sobol', *J. Nano Electron. Phys.* 7 No 4, 04027 (2015).
6. O.V. Sobol', *Phys. Solid State* 49 No 6, 1161 (2007).
7. N.A. Azarenkov, O.V. Sobol', V.M. Beresnev, A.D. Pogrebnjak, D.A. Kolesnikov, P.V. Turbin, I.N. Toryanik, *Metallofiz. Noveishie Tekhnol.* 35 No 8, 1061 (2013).
8. A.W. Bowman, A. Azzalini, *Applied Smoothing Techniques for Data Analysis* (New York: Oxford University Press: 1997).
9. R.J. Nemanich, S.A. Solin, *Phys. Rev. B* 20, 392 (1979).
10. C. Thomsen, S. Reich, *Phys. Rev. Lett.* 85, 5214 (2000).
11. A.C. Ferrari, J.C. Meyer, V. Scardaci, C. Casiraghi, M. Lazzeri, F. Mauri, S. Piscanec, D. Jiang, K.S. Novoselov, S. Roth, A.K. Geim, *Phys. Rev. Lett.* 97, 187401 (2006).
12. A.C. Ferrari, *Solid State Commun.* 143, 47 (2007).
13. P.K. Chu, L. Li, *Mater. Chem. Phys.* 96, 253 (2006).
14. A.W. Tsen, L. Brown, R.W. Havener, J. Park, *Account. Chem. Res.* 46, 2286 (2013).
15. X. Li, W. Cai, J. An, S. Kim, J. Nah, D. Yang, R. Piner, I. Jung, E. Tutuc, S.K. Banerjee, L. Colombo, R.S. Ruoff, *Science* 324, 1312 (2009).
16. A.A. Potapov, V.V. Bulavkin, V.A. German, O.F. Vyacheslavova, *ZhTF* 75 No 5, 28 (2005).
17. S.S. Al-Amri, N.V. Kalyankar, S.D. Khamitkar, *J. Comput.* 2 No 5, 83 (2010).